

Simulation and design of a LPGFS system for detection of *Escherichia coli* bacteria infestation in milk

D. SAVASTRU, S. MICLOS, R. SAVASTRU, I. LANCRANJAN*

National Institute of R&D for Optoelectronics - INOE 2000, 409 Atomistilor St., Magurele, Ilfov, RO-077125, Romania

The paper presents simulation results to be used for improved design of a portable short time response bio-sensor device dedicated to dairy industry for early detection of possible infestation with pathogen bacteria *Escherichia coli* and/or other micro-organisms in milk. A two-component model was developed: the first component is defined on computational biochemistry basis and refers to the quantitative definition of life cycle of bacteria or other type of micro-organisms while the second optimizes the constitutive characteristics of the Long Period Grating Fiber Sensors. The model predicts the modifications of the refractive index of the milk due to the presence of the bacteria and provides information about its concentration.

(Received November 13, 2018; accepted November 29, 2018)

Keywords: Fiber grating optical sensors, Refractive index measurement, Biochemical sensing

1. Introduction

The measurement of important chemical and biological parameters, such as composition and related compound concentrations, density, aggregation state and temperature in diversified environments is an important issue for various research, industrial, environment protection, biotechnology and medical applications [1-21]. For example, in the case of air and water quality control, the on-line monitoring of chemical compounds (e.g. greenhouse gases) and biological agents (e.g. toxins, bacteria), respectively, is crucial. This is a common issue as well for dairy/milk processing, pork meat processing, sheep meat, whether meat, poultry meat processing industry [1-14]. In several industrial circumstances, namely in anaerobic digesters, aquaculture tanks, the real-time monitoring of chemical parameters is critical.

Unfortunately, in a wide variety of situations, adequate technology is not available, or the employed techniques often require sample pre-treatment and are time consuming. Long waiting times between sample collection and processing results often compromise any time effective corrective actions. In this context, a real-time technology will be a very valuable tool.

A potential technology that will offer this benefit is optical fiber based, and is based on refractometric sensing. Optical fiber based refractometric sensing devices are a solution to these problems [9-12]. Among these optical fiber sensing devices LPGFS (Long Period Grating Fiber Sensors) with operation based on evanescent light field interaction with the ambient represent a newly appeared one with increased expansion class [9-20]. This technology has many benefits that makes it a promising

alternative solution to standard technologies: high sensitivity, immunity to electromagnetic interferences, chemically and biologically inert, small size, and capability for in-situ, real-time, remote, and distributed sensing are some of the most appealing characteristics that motivate a growing scientific community. All these above-mentioned facts lead to the necessity of designing real-time, in-line sensors, able to perform accurate measurements of chemical and biological parameters in short time on the minute time scale [7-12].

The design of such LPGFS devices for measuring chemical and biological parameters relies on proper modeling of light guided propagation through optical fiber core and on choosing the proper pitch of the grating [21-28]. Another important purpose of the modeling is the analysis of the evanescent field interaction with the ambient [21-45].

In this paper we discuss the simulation and design of an LPFGS sensor for detecting *E. coli* infestation in milk.

A special care is allocated for new design approaches applied in order to overcome cross sensitivity effects between several parameters to be measured, especially from temperature [21-45]. Another important task of the performed simulations consists of investigating LPGFS interrogation schemes, their implementation and characterization, with related virtual instrumentation for refractometric sensing devices [46-63].

The developed simulation model presented in the paper has two components. One component of the two previously mentioned is defined on computational biochemistry basis and refers to the quantitative definition of functional cycle of bacteria or other type of micro-organism under investigation [17-20]. From this first

model there are obtained concentrations of enzymes, polysaccharides, lipids and others which are generated by the investigated micro-organism. In the same time this biochemistry-based model gives information concerning the substances, mostly chemical elements absorbed by the micro-organism. The second component of the investigated simulation model has the task to optimize the constitutive characteristics of one or two Long Period Grating Fiber Sensors (LPGFS) used simply as it is or in interferometric Mach-Zehnder in-fiber setups such as cascade or twins' arrangements [21-46]. The second simulation model has an important feature: it is developed for the case of an ambient of the LPGFS with a refractive index value higher than that of the fiber cladding. As an exemplification there are presented the results obtained in the case of detection of bacteria Escherichia coli placed in milk.

Nevertheless, while optical fiber sensing technology is already in the market, this is mostly true for the measurement of physical parameters such as strain or vibration in structural health monitoring applications. In this regard, the measurement of bio-chemical parameters is intrinsically more complex as it typically requires interaction of light with the measurand in a gaseous or liquid phase. Therefore, a great deal of challenges is still at hand making this a fertile research field.

2. Theory

2.1. Simulation model of Escherichia coli

Brief remarks concerning the Escherichia coli bacterium. Escherichia coli (denoted also as E. coli) is a Gram-negative, facultative aerobic, rod-shaped, coliform bacterium of the genus Escherichia. Escherichia coli is commonly found in the lower intestine of warm-blooded organisms (endotherms). There are indexed about forty E. coli strains of which most are harmless, but with ten exceptions [2-8].

Among pathogenic bacteria, E. coli has a particular important place because of its enormous population of different bacterial strains which exhibit a very high degree of both genetic and phenotypic diversity. E. coli has many bacterial strains, over 40, four of them, K12, B, C, and W being thought of as model organism strains. It must be underlined that only 20 % of the genes in a typical E. coli genome are shared among all strains.

Another characteristic of E. coli model organism strains worth to be emphasized consists in its chemical type: it is chemoheterotrophic, unable to fix carbon to form their own organic compounds, utilizing organic energy sources such as carbohydrates, lipids, and proteins for reproduction. Among the E. coli bacterial strains, the most dangerous is the Escherichia coli O157:H7 one. It is known as E. coli EHEC strain. O157:H7 is an enterohemorrhagic serotype E. coli which causes severe,

fatal illness, typically through consumption of contaminated and raw food such as raw milk, meat and/or vegetables [10-21].

Brief remarks concerning the E. coli biochemistry simulation model. The E.coli model was developed based on a commercial software package, namely MATLAB 8.9, for quantitatively defining the functional cycle of E. coli bacterium under investigation [13, 17]. In the structure of the bulk of the developed computational biochemistry simulation model enters 274 routines and sub-routines with 55545 lines of program code which allows evaluation of an optimal path from several known possible chemical reactions involving the biochemical compounds previously known as possible being in the composition of the investigated E. coli bacterium strain. For a given set of ambient conditions, from the computational biochemistry simulation model of an investigated E. coli bacterium strain there are obtained concentrations of enzymes, polysaccharides, lipids, fatty acids, proteins and other biochemical compounds which are generated/interchanged with the ambient by the micro-organism under investigation. This means concentrations of an E. coli bacterium strain biochemical compounds at every moment of its functional cycle. Each of an E. coli bacterium strain biochemical compounds has optical (refractive index) and spectroscopically characteristic parameters which finally allows accurate identification using optical detection devices such as LPGFS.

There are five infrared (IR) spectral windows which were considered in connection with the developed computational biochemistry simulation model. The first window, situated between 3000 and 2800 cm^{-1} , contains C-H stretching vibrations of CH, CH₂ and CH₃ in the functional groups of membrane fatty acids and of amino acid side-chains, the second window, situated between 1800 and 1500 cm^{-1} , contains C=O stretching vibrations of amides linked to proteins, N-H deformation of amides linked to proteins, >C=O stretching vibrations of the ester groups in lipids and >C=O, >C=N, >C=C< stretching of the DNA or RNA bases, the third window, situated between 1500 and 1200 cm^{-1} , contains >CH₂ and -CH₃ bending modes, the fourth window, situated between 1200 and 900 cm^{-1} , contains symmetric stretching vibrations of PO⁻² groups in nucleic acids C-O-C and C-O-P stretching of carbohydrates and poly-saccharides in the cell membrane and the fifth window, situated between 900 and 700 cm^{-1} , contains aromatic ring vibrations of aromatic amino acids [16-20]. The life cycle of the E. coli bacterium nucleus simulation model, bacterium considered to have 20 % of the genes common to all E. coli strains, is presented schematically in [9]. This means that the chemical reactions specific to the E. coli bacterium nucleus simulation model involves 792 bio-chemical compounds [9-12]. There are considered 1057 possible chemical reactions [9-12].

In the case of *E. coli* detection when infesting milk using a LPGFS a specific issue arises, namely that of the milk as the ambient of the investigated measurement process [13-14]. Basically, the LPGFS is exploited as a refractometer which accomplishes a measurement of the refractive index of the ambient where the LPGFS is mounted. Therefore, an accurate value of milk refractive index must be considered. Since milk can be thought as water into which fat is dissolved at different concentrations, the value of its refractive index depends on fat content concentration [13, 15-17].

2.2. LPGFS simulation model

The structure of the detection setup incorporating a LPGFS is presented schematically in Fig. 1. The sensing component, the LPGFS is incorporated into a single mode (SM) optical fiber by inducing a permanent spatial modulation of the light propagation characteristics over a length L . The permanent spatial modulation represents an equivalent periodic perturbation of n_{core} of the fiber core refractive index, typically with a period of between 1 μm and 1000 μm , constituting a diffraction grating denoted as Long Period Grating (LPG). LPG causes light propagating through the optical fiber core as the fundamental mode to be coupled by scattering to the cladding light co-propagating modes which constitutes a discrete set. The coupling process represents energy transfer from light fundamental mode propagating through the core to the cladding co-propagating modes for which the Bragg resonance condition is fulfilled [21-35]. It is necessary to emphasize that the term copropagating modes refers to light propagation in the same sense. The energy transferred from the fundamental propagation mode is lost from it [36-45]. For the LPGFS operation one important feature deduced from this analyzes consists in the fact that the Bragg resonance condition imposes a discrete set of cladding modes which can be coupled by the grating with the core fundamental mode [46-63].

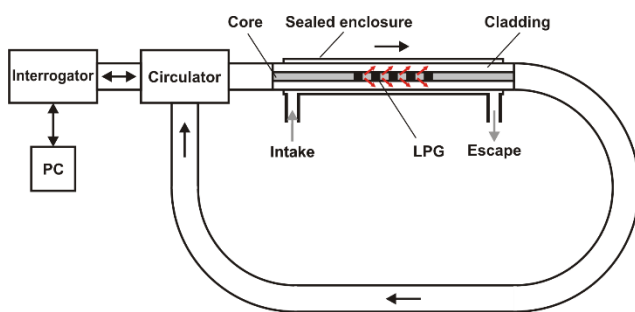


Fig. 1. Schematic representation of a LPGFS and its operation mode.

As can be observed in Fig. 1, the light beam having an input spectrum which is generated by a broadband source incorporated into a PC commanded interrogator is coupled through the circulator into the optical fiber core through which it is propagating as the fundamental mode until it is incident on LPG at blazing angle. LPG scattering process induces the energy transfer (an energy loss) from the fundamental mode to higher modes co-propagating through the optical fiber [21-61]. The cladding co-propagating modes are divergent at different angles from the optical fiber axis. Lower angle of divergence is equivalent to propagation in a volume closed to the core from where light can be coupled back to the fundamental mode when incidence on another LPG is accomplished. In Fig. 1 it is important to notice that the milk under investigation if it is or not contaminated with *E. coli* bacterium is flowing over the outer surface of the cladding through the intake, sealed enclosure and escape. For higher values of divergence angle of the light energy lost from the fundamental mode is transported to the cladding external surface [26-61]. At this point of analysis, it is worth to observe that the SM optical fiber zone containing the LPG has no mechanical PMMA protective layer [26-61]. Therefore, in this zone, the SM optical fiber cladding is in direct contact with the ambient into which the LPGFS is mounted, in our case, the milk possible infested with *E. coli* bacteria. This LPGFS constructive characteristic is very important for their use as chemical sensors, which is the investigated case. It is essential to notice that the energy lost from the fundamental mode by coupling on the LPG with the cladding co-propagating modes is observed as absorption bands located into the transmission spectrum of the LPG. According to Fig. 1, the LPG transmission spectrum is transmitted through the circulator back to the interrogator where it is analyzed and recorded.

The energy transfer characteristic absorption bands maxima are located at discrete wavelengths λ^i defined by the Bragg resonance condition [26-41]:

$$\lambda^i = (n_{eff}^i - n_{clad}^i) \cdot \Lambda \quad (1)$$

where λ^i is the peak wavelength of the absorption band observed in the LPGFS transmission spectrum which corresponds to the i^{th} cladding propagation mode, n_{eff}^i is the effective value of the refractive index of the optical fiber core, n_{clad}^i is the refractive index effective value of the i^{th} possible cladding propagation mode and Λ is the period of the LPG. For a clearer analysis it is useful to observe from a mathematical point of view that for both effective values of refractive index of core and cladding propagation modes there are only numerical solutions obtained by solving the equations of electromagnetism theory, equations which imply the ambient refractive index. Equation (1) is useful for sensing observing that the

effective values of refractive index of core and cladding modes depend on the ambient refractive index [27-45]. Any infinitesimal modification of the ambient refractive index represents a change in characteristics of light propagation through the LPGFS and is sensed by the LPG by observing the spectral shifting and broadening of each absorption bands induced in optical fiber transmission spectrum [30, 33-37, 46-57].

It is worth to underline that Equation (1) is obtained considering the coupling by LPG scattering of fundamental mode of light guided propagation through the optical fiber core to the cladding co-propagating modes as the single interaction between optical fiber modes. This is an acceptable or not approximation depending on the difference between the refractive index values of the ambient and cladding and on the optical quality of the external surface of optical fiber commonly made of fused silica. For detection of pathogen bacteria such as some of *E. coli* strains which are placed in water or milk as ambient are it is often necessary to improve LPGFS sensitivity. The starting point for this improvement consists in using a modified version of Equation (1) namely [27, 30, 46-50]

$$\lambda^i = (n_{eff}^i - n_{clad}^i) \Lambda + (\kappa_{c-c} - \kappa_{cl-cl}) \quad (2)$$

where λ^i , n_{eff}^i and n_{clad}^i have the same significance while κ_{c-c} and κ_{cl-cl} are the self-coupling coefficients of the core mode and the cladding mode, respectively. Equation (2) expresses mathematically that a small fraction of the cladding mode field, the evanescent field, travels outside the optical fiber, into the ambient interacting with it, changing the n_{clad}^i and thus changing the λ^i . The LPGFS sensing principle relies on measuring the changes in λ^i , the smaller the period of refractive index variation (Λ) the larger would be cladding mode evanescent field leading to high sensitivity. It is a thin line between the domains where Eq. (1) or Eq. (2) is enough accurate to be used instead of the other. It can be justified theoretically that the sensitivity to ambient refractive index of LPGFSs, more precisely of the LPG, can be increased up to 2500 nm/r.i.u. which is enough for *E. coli*. A more carefully investigation of the *E. coli* detection process reveals that the *E. coli* biochemical compounds interactions between them and/or with the optical fiber material on the LPG surface changes the ambient refractive index. This specific process in turn causes the Bragg resonance center wavelength down shifts of the LPG. The wavelength shifts are measured and are a measure of the bacteria concentration [26-61]. To achieve maximum sensitivity of the LPG it is made in a way that its turning point is around the refractive index of water in which the bacteria is to be detected. This is done by deliberate controlled etching of the LPG. However, if *E.*

coli is to be measured in milk, then it matters what the refractive index of milk is and how it varies with fat content [13, 15-17].

3. Simulation results

The simulation of a LPGFS device which is designed to detect *E. coli* infesting milk is performed in two main stages each having several sub-stages with the final task to obtain the spectral shift of a characteristic absorption band induced in the LPGFS transmission spectrum. The first major stage consists of defining the LPGFS spectral parameters. The second major stage consists in obtaining spectral information concerning the *E. coli* specific biochemical compounds and their spectroscopic parameters. There is an interaction between these two main stages. In this sense it must be underlined that *E. coli* specific biochemical compounds spectroscopic parameters are used for defining the one up to five points of interest to be investigated in the LPGFS output according to the five spectral windows specified in Section 2.

The first step of the first main stage consists in defining the geometrical and refractive index parameters of the SM optical fiber into which the grating is manufactured. For Corning SMF 28e and Fibercore SMF 750 optical fibers the parameters are: core radius = 2.8 μm , core refractive index = 1.4589, cladding radius = 62.5 μm , cladding refractive index = 1.4557 and cut-off wavelength = 650 nm [30, 39-46]. These two SM optical fibers imposed on the market as standard for communications and sensing devices manufacturing. A special mention refers at the value of the optical fiber ambient refractive index. The refractive index water is 1.3352. It was considered that water is the milk main component. During simulations several fat concentrations as dissolved in water were considered. According to literature there is no Sellmeier analytical relation for water, only tabulated numerical data. Implicitly, in the case of milk the situation is the same. Without reducing the generality of the approach of the numerical method, for the performed simulations a constant value of milk with a fat concentration of 3.5 % refractive index of 1.3810 was used. This agrees with the data presented in literature [36-47, 50-63].

Another issue of interest which was investigated consists in whether to consider or not a constant value of optical fiber core refractive index. In Figs. 2 and 3 there are presented the dispersion curves of fused silica doped with Ge 3.5 % and 5.8 % concentrations [21, 30].

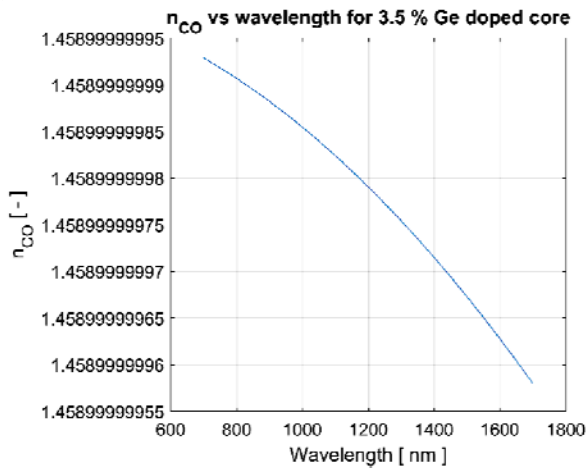


Fig. 2. Dispersion curve of fused silica doped with Ge at 3.5 % concentration.

The dispersion curves are defined using Sellmeier equation with coefficients obtained from Corning. Corning uses the technique of doping the fused silica with Ge for manufacturing the optical fiber core with a refractive index value slightly larger than that of the cladding. It can be observed that the variation with wavelength in the spectral domain of interest of the optical fiber core refractive index value is very low, only the sixth or seventh decimal figure being different with wavelength. In consequence, during simulations, a constant value of optical fiber core was considered, namely that observed for Ge doping at 3.5 % concentration.

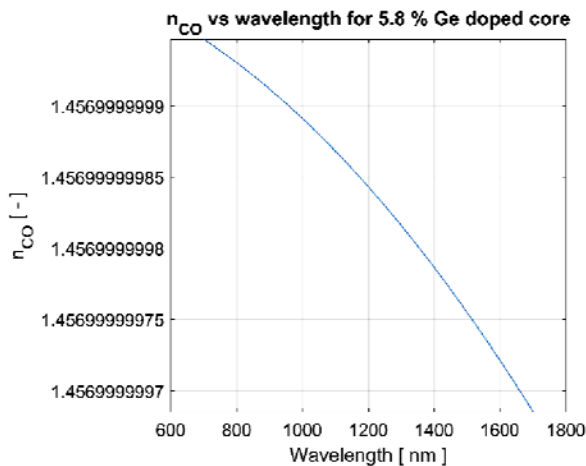


Fig. 3. Dispersion curve of fused silica doped with Ge at 5.8 % concentration.

The second step of the first main stage consists in evaluation of the LPGFS parameters. This is accomplished using Eq. (1) or (2). At the end of this step the characteristic phase matching curves (PMC) are obtained. It must be observed that for a given LPGFS the PMC are a set of parametric bidimensional curves each of them representing a light mode of propagation through the optical fiber. Each point of such a curve represents a pair of light wavelength and grating period (Λ_{LPG}) satisfying

the Bragg resonance condition. This means that for a fixed Λ_{LPG} the points on the PMC set are the wavelengths λ^i where are located the peaks of the absorption bands existing in the LPGFS transmission spectrum. PMC are used afterwards for correlating the E. coli biochemical compounds characteristic spectroscopic data with the wavelengths at which the spectral shifts of the absorption bands of LPGFS transmission spectra will be observed [21-57].

Firstly, there will be defined the inputs of Eqs. (1) and (2), namely the refractive index effective values of the core and cladding propagating modes, n_{eff} and n_{clad}^i which are obtained by numerically solving the equations of light propagation through the optical fiber. The formulation of these equations depends on the geometrical and refractive index parameters of the SM optical fiber into which the grating is manufactured. In Figs. 4 and 5 are presented the simulation results obtained for the n_{eff} and n_{clad}^i variations versus light wavelength in the investigated system. n_{eff} and n_{clad}^i are calculated using a three layers model of the optical fiber - the optical fiber core and cladding are the first two layers and the ambient is the third one. This is the point of the simulation process where the ambient intervenes directly. It must be mentioned that in Fig. 5 there are presented the variations of the light modes propagating through the optical fiber cladding with the largest possible divergence angle from the optical axis, i.e. near the optical fiber cladding outer surface. These cladding light modes are important for LPGFS applications in biochemistry, i.e. for detection of E. coli pathogen bacteria. The absorption bands in the LPGFS transmission spectra corresponding to these light propagation modes are broaden with the largest full width half measure (FWHM) of this kind of absorption bands.

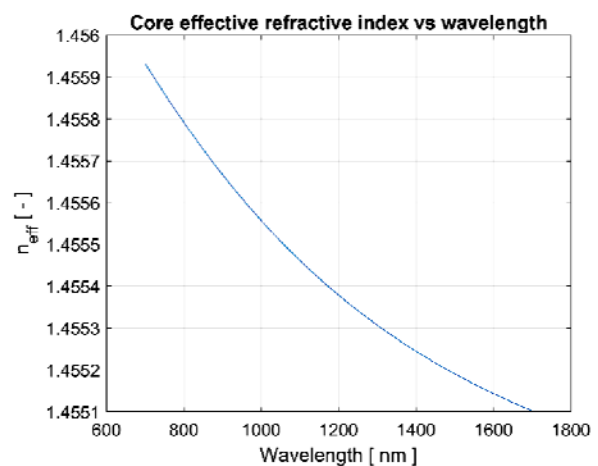


Fig. 4. Variation of SM optical fiber core effective value of refractive index n_{eff} vs light wavelength.

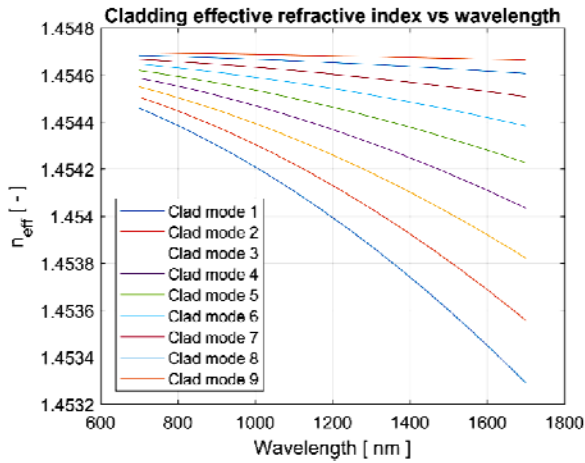


Fig. 5. Variations of the SM optical fiber cladding effective value of refractive index n_{clad}^i (n_{eff} in figure) vs light wavelength of nine cladding modes.

In Figs 6 - 9 there are presented the simulation results obtained for PMC using Eqs. (1) and (2). In Figs. 6 (using Eq. (1)) and 8 (using Eq. (2)) there are presented PMC as (wavelength, Λ_{LPG}) parametric curves. In Figs. 7 (using Eq. (1)) and 9 (using Eq. (2)) there are presented PMC as (wavelength, Λ_{LPG}) parametric curves. For both Eqs. (1) and (2) simulation results obtained for PMC are presented in two alternative variants of analyzing PMC as parametric curves. The comments referring at LPGFS operation mode become clear after the significance of the PMC is carefully analyzed. It appears that the following simple procedure is applicable: in the plots presented in Figs. 6 - 9 imagine a horizontal or vertical line, i.e. corresponding to a given value of Λ_{LPG} or light wavelength; the intersection points of this horizontal or vertical line with the phase matching curves defines the peaks λ^i of absorption bands appearing in the LPGFS transmission spectrum. In the case of E. coli infesting milk detection using LPGFS, for a given Λ_{LPG} , is chosen a λ^i situated in the vicinity of the peak wavelength corresponding to a maximum absorption band of the transmission spectrum of a biochemical compound characteristic of E. coli. For detection of a given E. coli strain using a given LPGFS, by choosing one or several, at least five uniquely characteristic biochemical compounds for the given E. coli strain, compounds which have transmission spectra with absorption bands situated in the five spectral windows, it becomes possible to find a set of minimum one λ^i corresponding to fulfilment of Bragg resonance condition for the given LPGFS. It must be observed that at this point of the simulation process the role of the E. coli life cycle simulation model is important and evident by providing the information concerning the E. coli characteristic biochemical compounds. E. coli life cycle simulation model provides also the concentrations of the bacteria biochemical compounds at every moment, a detail important for defining the E. coli bacteria status, dead or alive. In the case of E. coli bacteria infesting milk special care should be taken for avoiding the situation of bio-chemical compounds common to the milk and E. coli.

In Fig. 10 there are presented the simulation results obtained for observing the spectral shifts of the absorption bands peaks caused by the milk infestation with E. coli. It was considered the case of milk with a concentration of 3.5 % fat substances, at room temperature. It was investigated an absorption band specific to a E. coli biochemical compound of lipopolysaccharide type.

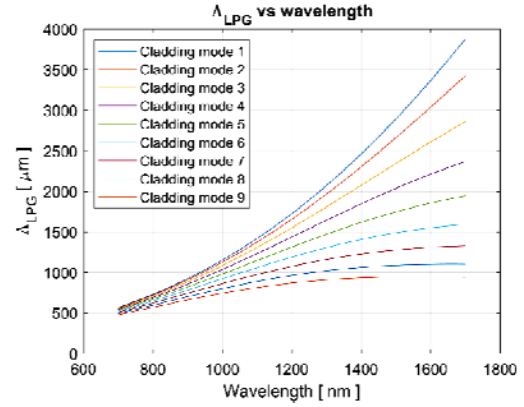


Fig. 6. The PMC obtained using Eq. (1) of the investigated LPGFS represented as Λ_{LPG} vs wavelength parametric curves for nine cladding light modes.

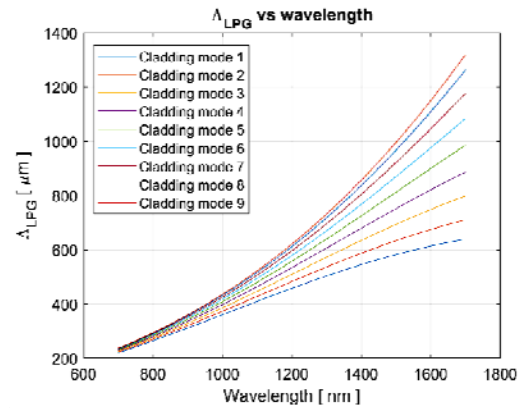


Fig. 7. The PMC obtained using Eq. (2) of the investigated LPGFS represented as Λ_{LPG} vs wavelength parametric curves for nine cladding light modes.

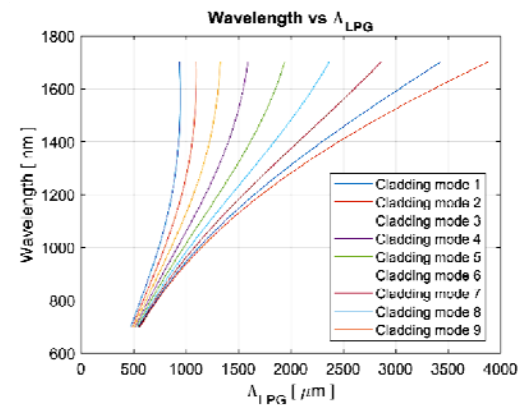


Fig. 8. The PMC obtained using Eq. (1) of the investigated LPGFS represented as wavelength vs Λ_{LPG} parametric curves for nine cladding light modes.

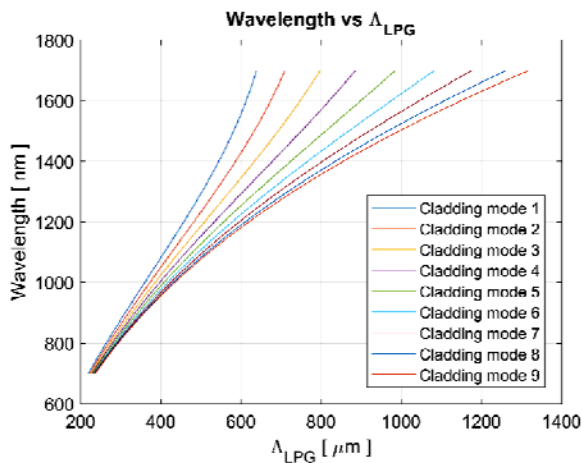


Fig. 9. The PMC obtained using Eq. (2) of the investigated LPGFS represented as wavelength vs Δ_{LPG} parametric curves for nine cladding light modes.

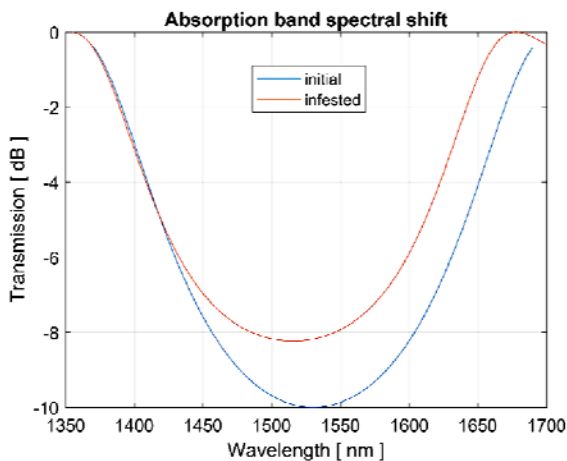


Fig. 10. The simulated spectral shift of LPGFS absorption band induced by the *E. coli* infestation of milk.

The maximum absorption band of the *E. coli* biochemical compound is situated at 1535.5 nm. It was considered a concentration of *E. coli* bacteria of 5×10^7 cfu/ml, cfu being the acronym of Colony Forming Units, a unit for quantification of pathogen bacteria concentration. The value of λ^i for Bragg resonance condition was 1530.0 nm. As expected, a slight increase of ambient refractive index was observed causing a spectral shift of λ^i down to 1515.5 nm. According to the simulation there was a decrease of full width half measure bandwidth (FWHM) from 218.3 nm to 211.5 nm. The value of *E. coli* bacteria concentration is deduced implicitly through the concentration of the observed lipo-polysaccharide.

4. Conclusions

In conclusion, the simulation approach presented in this paper opens a new pathway for the design of LPGFS for *E. coli* detection in infested milk. The new design

method can be used, with the necessary changes, for the detection of other pathogen bacteria or germs. The accuracy of the detection method can be largely improved by imposing an enlarged number of specific spectral identification points.

Also, on the basis of the presented newly developed simulation method consisting in analyzing correlation of biochemical characteristics of biological tissue cell with its optical ones, further developments such as detection of tuberculosis, nosocomial infections or various cancer forms using LPGFS devices becomes possible.

Acknowledgments

This work was supported by the MANUNET grant MNET17/NMCS0042 and by the Core Program project no. PN 18 28.01.01.

References

- [1] A. Feist, C. Henry, J. Reed, M. Krummenacker, A. Joyce, P. Karp, et al., *Mol. Syst. Biol.* **3**(1), 121 (2007).
- [2] M. Zourob, S. Mohr, B. J. Brown, P. R. Fielden, M. B. McDonnell, N. J. Goddard, *Biosens. Bioelectron.* **21**(2), 293 (2005).
- [3] A. Shabani, M. Zourob, B. Allain, C. Marquette, M. Lawrence, R. Mandeville, *Anal. Chem.* **80**(24), 9475 (2008).
- [4] A. D. Taylor, Q. Yu, S. Chen, J. Homola, S. Jiang, *Sensor. Actuat. B-Chem.* **107**(1), 202 (2005).
- [5] B. Van Dorst, J. Mehta, K. Bekaert, W. De Coen, P. Dubruel, et al., *Biosens. Bioelectron.* **26**(4), 1178 (2010).
- [6] S. Balasubramanian, I. Sorokulova, V. Vodyanoy, A. Simonian, *Biosens. Bioelectron.* **22**(6), 948 (2007).
- [7] V. Nanduri, I. B. Sorokulova, A. M. Samoylov, A. L. Simonian, V. A. Petrenko, V. Vodyanoy, *Biosens. Bioelectron.* **22**(6), 986 (2007).
- [8] M. J. Archer, J. L. Liu, *Sensors* **9**(8), 6298 (2009).
- [9] I. Abdulhalim, M. Zourob, A. Lakhtakia, *Electromagnetics* **28** (3), 214 (2008).
- [10] D. J. Monk, D. R. Walt, *Anal. Bioanal. Chem.* **379**(7-8), 931 (2004).
- [11] I. Gogol, *Vet. Med. Nauki.* **15**, 82 (1978).
- [12] A. H. Soomro, M. A. Arain, M. Khaskheli, B. Bhutto, *Pak. J. Nutrition* **1**(3), 151 (2002).
- [13] R. Kumar, A. Prasad, *Veterinary World* **3**(11), 495 (2010).
- [14] K. Miyajima, T. Koshida, T. Arakawa, H. Kudo, H. Saito et al., *Anal. Bioanal. Chem.* **379** (7-8), 931 (2004).
- [15] T. Geng, Joe Uknalis, S.-I Tu, A. K. Bhunia, *Biosensors* **3**(1), 120 (2013).
- [16] V. Nanduri, S. Balasubramanian, V. Vodyanoy, A. Simonian, S. Sista, *Anal. Chim. Acta* **589**(2), 166 (2007).

- [17] P. Arora, A. Sindhu, N. Dilbaghi, A. Chaudhur, *Biosens. Bioelectron.* **28**(1), 1 (2011).
- [18] Y. M. Bae, B. K. Oh, W. Lee, W. H. Lee, J. W. Choi, *Biosens. Bioelectron.* **20**(4), 895 (2004).
- [19] A. J. Baeumner, R. N. Cohen, V. Miksic, J. M. Min, *Biosens. Bioelectron.* **18**(4), 405 (2003).
- [20] S. P. Chandran, S. Hotha, B. L. V. Prasad, *Curr. Sci.* **95**(9), 1327 (2008).
- [21] S. W. James, R. P. Tatam, *Meas. Sci. Technol.* **14**(5), R49 (2003).
- [22] T. Erdogan, *J. Opt. Soc. Am. A* **14**(8), 1760 (1997).
- [23] T. Erdogan, *J. Lightwave Technol.* **15**(8), 1277 (1997).
- [24] A. I. Kalachev, V. Pureur, D. N. Nikogosyan, *Opt. Commun.* **246**(1-3), 107 (2004).
- [25] C. S. Cheung, S. M. Topliss, S. W. James, R. P. Tatam, *J. Opt. Soc. Am. B* **25**(6), 897 (2008).
- [26] J. M. Lopez-Higuera, L. R. Cobo, *J. Lightwave Technol.* **29**(4), 587 (2011).
- [27] J. F. Akki, A. S. Lalasangi, P. U. Raika, T. Srinivas, L. S. Laxmeshwar, U. S. Raikar, *IOSR-JAP* **4**(3), 41 (2013).
- [28] Y. Koyamada, *IEEE Photonic. Tech. L.* **13**(4), 308 (2001).
- [29] S. Kher, S. Chaubey, J. Kishore, S. M. Oak, *IEEE Sens. J.* **13**(11), 4482 (2013).
- [30] R. Kashyap, *Fiber Bragg Gratings*, Academic Press, 2009.
- [31] P. Biswas, N. Basumallick, S. Bandyopadhyay, K. Dasgupta, A. Ghosh, S. Bandyopadhyay, *IEEE Sens. J.* **15**(2), 1240 (2015).
- [32] S. Chaubey, S. Kher, J. Kishore, S. M. Oak, *Pramana* **82**(2), 373 (2014).
- [33] S. Chaubey, S. Kher, S. M. Oak, 7th Workshop on Fiber and Optical Passive Components (WFOPC), Montreal, Canada, 13-15 July 2011, 1-4.
- [34] X. Lan, Q. Han, J. Huang, H. Wang, Z. Gao et al., *Sens. Actuators B Chem.* **177**, 1149 (2013).
- [35] X. Lan, Q. Han, T. Wei, J. Huang, H. Xiao, *IEEE Photonic. Tech. L.* **23**(22), 1664 (2011).
- [36] S. Kher, S. Chaubey, R. Kashyap, S. M. Oak, *IEEE Photonic. Tech. L.* **24**(9), 742 (2012).
- [37] V. Mishra, S. C. Jain, N. Singh, G. C. Poddar, P. Kapur, *Indian J. Pure Ap. Phy.* **46**, 106(2008).
- [38] A. Iadicicco, D. Paladino, P. Pilla, S. Campopiano, A. Cutolo, A. Cusano, Ch. 14: Long Period Gratings in New Generation Optical Fibers. In: M. Yasin, S. W. Harun, H. Arof, Eds., *Recent Progress in Optical Fiber Research*, InTech, 291 (2012).
- [39] F. Chiavaioli, P. Biswas, C. Trono, A. Giannetti et al., *Biosens Bioelectron* **60**, 305 (2014).
- [40] R. Garg, S. M. Tripathi, K. Thyagarajan, W. J. Bock, *Sens. Actuators B Chem.* **176**, 1121 (2013).
- [41] T. Allsop, K. Kalli, K. Zhou, Y. Lai, G. Smith et al., *Opt. Commun.*, **281**(20), 5092 (2008).
- [42] J. Kanka, *Proc. SPIE* **8426**, 34 (2012).
- [43] J. Kanka, *Sens. Actuators B Chem.* **182**, 16 (2013).
- [44] X. Shu, X. Zhu, Q. Wang, S. Jiang, W. Shi, Z. Huang, *Electron. Lett.* **35**(8), 649 (1999).
- [45] M. Smietana, M. Koba, P. Mikulic, W. J. Bock, *Meas. Sci. Technol.* **25**(11), Article ID: 114001 (2014).
- [46] I. M. Ishaq, A. Quintela, S. W. James, G. J. Ashwell, J. M. Lopez-Higuera, R. P. Tatam, *Sens. Actuators B Chem.* **107**, 738 (2005).
- [47] S. Korposh, S. James, R. Tatam, S. W. Lee, Ch. 4: Optical Fiber Long-Period Gratings Functionalised with Nano-Assembled Thin Films: Approaches to Chemical Sensing, In: C. Cuadrado-Laborde, Ed., *Current Trends in Short- and Long-Period Fiber Gratings*, InTech, 63-86 (2013).
- [48] A. Cusano, A. Iadicicco, P. Pilla, L. Contessa, S. Campopiano, A. Cutolo, *Opt. Express* **14**(1), 19 (2006).
- [49] J. Yang, L. Yang, C. Q. Xu, Y. Li, *J. Lightwave Technol.* **25**(1), 372 (2007).
- [50] D. Savastru, S. Miclos, R. Savastru, I. Lancranjan, *Proc. SPIE* **9517**, 95172A (2015).
- [51] S. Miclos, D. Savastru, R. Savastru, I. Lancranjan, *Compos. Struct.* **183**(SI), 521 (2018).
- [52] D. Savastru, S. Miclos, R. Savastru, I. Lancranjan, *Compos. Struct.* **183**(SI), 682 (2018).
- [53] E. Anemogiannis, E. N. Glytsis, T. K. Gaylord, *J. Lightwave Technol.* **21**(1), 218 (2003).
- [54] S. Khaliq, S. W. James, R. P. Tatam, *Opt. Lett.* **26**(16), 1224 (2001).
- [55] K. O. Hill, B. Malo, F. Bilodeau, D. C. Johnson, *Annu. Rev. Mater. Sci.* **23**, 125 (1993).
- [56] S. Miclos, D. Savastru, I. Lancranjan, *Rom. Rep. Phys.* **62**(3), 519 (2010).
- [57] I. Lancranjan, S. Miclos, D. Savastru, *J. Optoelectron. Adv. M.* **12**(8), 1636 (2010).
- [58] I. Lancranjan, S. Miclos, D. Savastru, A. Popescu, *J. Optoelectron. Adv. M.* **12** (12), 2456 (2010).
- [59] R. Savastru, I. Lancranjan, D. Savastru, S. Miclos, *Proc. SPIE* **8882**, 88820Y (2013).
- [60] S. Miclos, D. Savastru, R. Savastru, I. Lancranjan, *Proc. SPIE* **9517**, 95172B (2015).
- [61] D. Savastru, S. Miclos, R. Savastru, I. Lancranjan, *Rom. Rep. Phys.* **67**(4), 1586 (2015).
- [62] R. Q. Lv, T. M. Zhou, L. B. Zhang, H. J. Peng, Y. N. Zhang, *Optoelectron. Adv. Mat.* **11**(11-12), 633 (2017).
- [63] D. Liu, G. Humbert, Y. Liu, D. Zhao, *Optoelectron. Adv. Mat.* **11**(5-6), 289 (2017).

*Corresponding author: ion.lancranjan@inoe.ro